Versatile UPQC Control System with a Modified Repetitive Controller under Nonlinear and Unbalanced Loads

Quoc-Nam Trinh[*] and Hong-Hee Lee[†]

[*]Energy Research Institute @ NTU, Nanyang Technological University, Singapore
[†]School of Electrical Engineering, University of Ulsan, Ulsan, Korea

Abstract

A standard repetitive controller (RC) is theoretically able to replace a bank of resonant controllers in harmonic signals tracking applications. However, the traditional RC has some drawbacks such as a poor dynamic response and a complex structure to compensate grid frequency deviations for an effective unified power quality conditioner (UPQC) control scheme. In order to solve these problems, an improved RC with an outstanding dynamic response and a simplified grid frequency adaptive scheme is proposed for UPQC control systems in this paper. The control strategy developed for the UPQC has delay time, i.e., one-sixth of a fundamental period ($T_p/6$), repetitive controllers. As a result, the UPQC system can provide a fast dynamic response along with good compensation performance under both nonlinear and unbalanced loads. Furthermore, to guarantee the excellent performance of the UPQC under grid frequency deviations, a grid frequency adaptive scheme was developed for the RC using a simple first order Padé's approximation. When compared with other approaches, the proposed control method is simpler in structure and requires little computing time. Moreover, the entire control strategy can be easily implemented with a low-cost DSP. The effectiveness of the proposed control method is verified through various experimental tests.

Key words: Active Power Filter, Harmonic Compensation, Repetitive Control, Unified Power Quality Conditioner

I. INTRODUCTION

In recent decades, the intensive use of power electronics devices and nonlinear loads such as diode rectifiers, adjustable speed motor drives, and switching power supplies has led to the injection of many harmonic currents into power distribution systems. Harmonic currents have various severe effects on power systems such as voltage distortions, increased losses and heat in networks, malfunctions of electronic equipment, and degraded power quality in networks. Therefore, the installation of power filters and power custom devices to improve power quality has become a mandatory requirement for both network operators and end users.

Various kinds of compensating devices have been proposed and developed in the literature. These devices include passive filters, shunt active power filters (APFs) [1], [2], and hybrid APFs [3], which mitigate current harmonics, and series APFs [4] and dynamic voltage restorers [5], which deal with voltage distortions and voltage sag compensation.

Recently, the unified power quality conditioner (UPQC), which is composed of shunt and series APFs, has been developed as an advanced and powerful compensation device to simultaneously deal with current and voltage related problems. Most of the previous UPQC control methods involve voltage sag/harmonic detectors and voltage/current controllers to provide different power quality improvement functions [6]-[10]. To avoid complex control schemes and hardware, many researchers have tried to implement UPQCs without harmonic extractors through advanced control schemes such as hysteresis controllers [11]-[14], artificial neural network and particle swarm optimization-based controllers [15], [16], and proportional-integral (PI) plus resonant controllers [17]. Among these methods, the resonant control approach offers the best control performance thanks

to its effectiveness in tracking harmonic signals. However, since each resonant controller effectively tracks only one specific frequency signal, a large number of resonant controllers are needed to regulate all of the concerned harmonic components. This makes the whole control scheme complex and bulky.

To simplify the complexity of multiple resonant controllers, the repetitive controller (RC) is one of the promising solutions. A single RC can replace a bank of resonant controllers to simultaneously compensate a large number of harmonic components. The RC has been widely applied to various power converter applications such as UPSs [19]-[21], active power filters [22], and grid-connected inverters [23]. Despite the effectiveness of the RC in harmonic compensation/rejection, the traditional RC regularly suffers from two main shortcomings: a poor dynamic response, which is due to a long delay time, i.e., one fundamental period; and deteriorated performance under system frequency variations, e.g., grid frequency deviations. To resolve the slow transient response of the traditional RC, a number of control approaches have been introduced where the RC is designed to compensate only the $(6n\pm1)$th ($n = 1, 2, 3\ldots$) harmonics, which reduces the time delay by six times [24]-[27]. However, under unbalanced load conditions, the performance of these RCs is diminished because they can only deal with $(6n\pm1)$th ($n = 1, 2, 3\ldots$) harmonic components, which is suitable for three-phase nonlinear loads.

On the other hand, to maintain the same performance of the RC despite grid frequency deviations, two main approaches have been introduced: adjusting the sampling period of the control system so that the number of delay samples, N, can be maintained as an integer value [28], [29]; or approximating the fraction delay term so that the RC can be accurately implemented even though N is a non-integer number [30]-[35]. The first solution is simple and easy to implement. However, it does not guarantee a good performance when the grid frequency variations increase. Furthermore, in the case where the sampling period is changed, the whole control system needs to be redesigned. The second solution, approximating the fraction delay term, can be achieved by a first order low pass filter (LPF) [30], a finite impulse response (FIR) filter [31], Linear interpolation [32], and Lagrange interpolation [33]-[35]. A LPF with a variable cut-off frequency is simple to implement. However, this method cannot ensure a good performance of the RC in the case of grid frequency variations because finding the relationship between the cut-off frequency of the LPF and the grid frequency deviation is quite challenging. On the other hand, FIR filters and Lagrange interpolation with adjustable coefficients are more complicated, consume long computational time and require high order FIR filters to guarantee an accurate approximation. Unfortunately, with a complex control system the RC is no longer simple compared to other control techniques.

In order to solve the above mentioned problems in the traditional RC, i.e., a poor dynamic response due to a long delay time and complexity in terms of compensating grid frequency deviations, this paper introduces a modified RC and the grid frequency adaptive method to implement a versatile UPQC control system. To overcome the slow dynamic response of the traditional RC, a new RC was developed with a reduced delay time, i.e., one-sixth of a fundamental period ($T_p/6$), so that the UPQC system can achieve approximately six times faster response than that of the traditional RC. In addition, by combining two RCs, the UPQC is able to achieve good performance under both nonlinear and unbalanced load conditions. Moreover, a simple grid frequency adaptive scheme is developed by using a first order Padé's approximation to maintain the same UPQC performance in spite of grid frequency deviations. Thanks to the simple control structure and reduced computation time of the Padé's approximation, the proposed control strategy is significantly simplified compared to other grid frequency adaptive algorithms. The proposed control algorithm can be easily implemented with low-cost DSPs such as TMS320F2812 of Texas Instruments. Finally, its feasibility is verified through various experimental tests.

II. PROPOSED CONTROL STRATEGY FOR THE UPQC

Fig. 1 shows the configuration of a three-phase UPQC connected with a utility grid and loads. The UPQC consists of two voltage source inverters connected back-to-back through a common DC-link capacitor, where one inverter is a shunt APF and the other inverter is a series APF. The series APF is connected in series between the supply and the load through a series transformer. Meanwhile, the shunt APF is connected in parallel with the loads through an inductor L_{sh}. An LC (L_f, C_f) filter is connected at the AC output voltage of the series APF to eliminate high-frequency switching noises. In Fig. 1, in order to deal with voltage and current related problems, the conventional control strategies require voltage sag/harmonic detectors and current/voltage controllers that must be designed properly to achieve good performance. As a consequence, a complex control system is often needed to fulfill the control objectives.

To overcome the complexity of the conventional control approaches and to enhance the control performance of the UPQC, an improved control strategy is suggested where modified RCs are used, as shown in Fig. 2. It can be seen in this figure that the RC voltage controller is designed in the series APF to compensate the load voltage to be sinusoidal despite voltage distortions at the supply side. Meanwhile, a PI-2RC current controller is developed in the shunt APF, so that the supply current is compensated to be balanced and
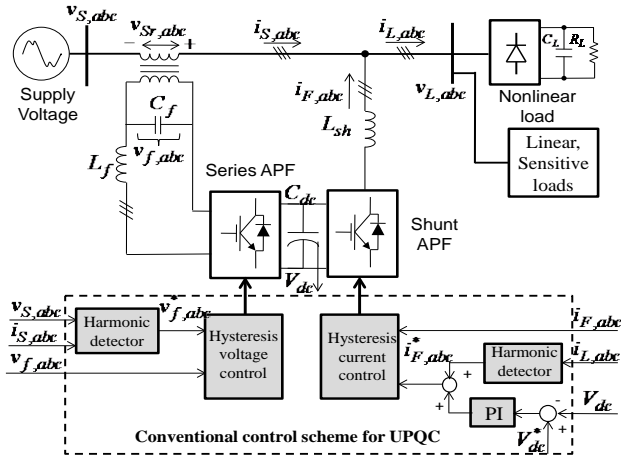
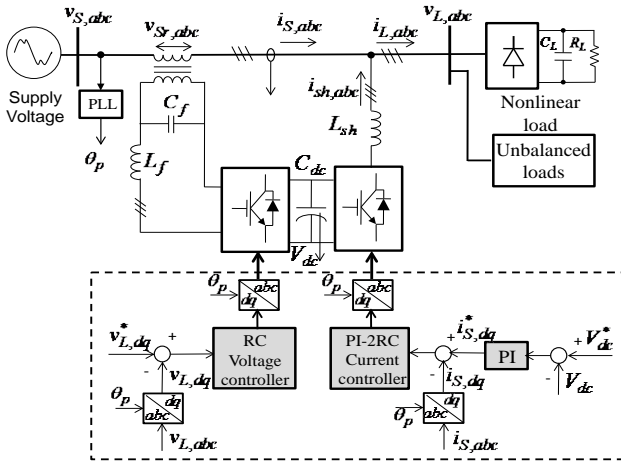Fig. 1. System configuration and traditional control strategy for UPQC.

Fig. 2. Proposed control strategy for UPQC.

sinusoidal in spite of current distortions/imbalances. The operating principles of the voltage and current controllers are explained in detail in the following sections.

A. Current Controller for the Shunt APF

If nonlinear loads are used in a system, as given in Fig. 2, the load current is composed of the fundamental component (i_{L1}) and harmonic components (i_{Lh}) as follows:

$$i_L = i_{L1} + i_{Lh} = I_{L1}\sin(\omega t - \theta_{L1})$$
$$+ \sum_{h \neq 1} I_{Lh}\sin(h\omega t - \theta_{Lh}). \qquad (1)$$

In order to compensate the supply current (i_S) to be sinusoidal and in-phase with the supply voltage (v_S), the traditional control methods regularly involve harmonic detection and current regulation stages [6], [7]. In this paper, a simplified control method is used wherein the supply current reference (i_S^*) is directly generated to be sinusoidal and in-phase with the supply voltage:
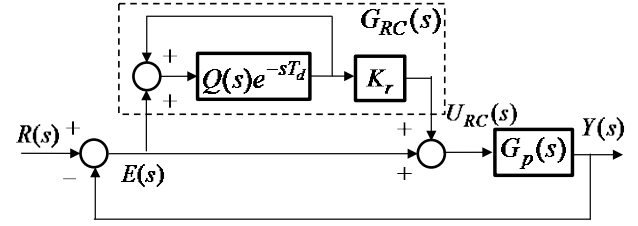
$$i_S^* = I_{S1}^* \sin \omega t \qquad (2)$$

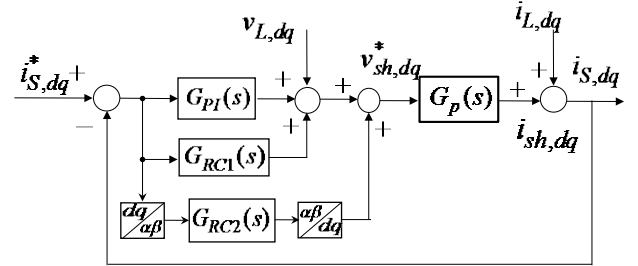Fig. 3. Block diagram of the traditional RC.

Fig. 4. Block diagram of the proposed PI-2RC current controller.

where I_{S1}^* is the amplitude of the supply current reference, which is determined by the outer DC-link voltage control loop.

This control method does not use a harmonic detector. Thus, the control performance of the shunt APF relies solely upon the current regulator. To achieve good compensation performance with the simplified current controller, this paper develops an advanced current controller with the aid of a PI controller and a modified RC. The traditional RC has characteristics similar to those of a bank of resonant controllers. It is able to simultaneously track a large number of harmonic currents/voltages [19]. A block diagram of the traditional RC is illustrated in Fig. 3 and the transfer functions of the PI controller and the RC in the continuous time domain are expressed in (3) and (4), respectively.

$$G_{PI}(s) = K_p + \frac{K_i}{s}, \qquad (3)$$

$$G_{RC}(s) = \frac{K_r Q(s) e^{-sT_d}}{1 - Q(s) e^{-sT_d}}, \qquad (4)$$

where K_p and K_i are the proportional and integral gains of the PI controller, respectively, T_d is the time delay of the RC, $Q(s)$ is the filter transfer function, and K_r is the RC gain.

Since the time delay T_d in (4) is selected to be the same as the fundamental period (T_p) of the supply voltage, the RC can compensate all of the harmonics (odd and even). However, it has a poor dynamic performance due to its long time delay [19]. To overcome this time delay problem, T_d is reduced six times to be $T_d = T_p / 6$. Although the dynamic response is significantly improve, this solution is only effective with the ($6n\pm1$)th (n=1, 2, 3…) harmonic components [24], [25]. Therefore, to achieve a fast transient response and effectiveness of the controller under abnormal load
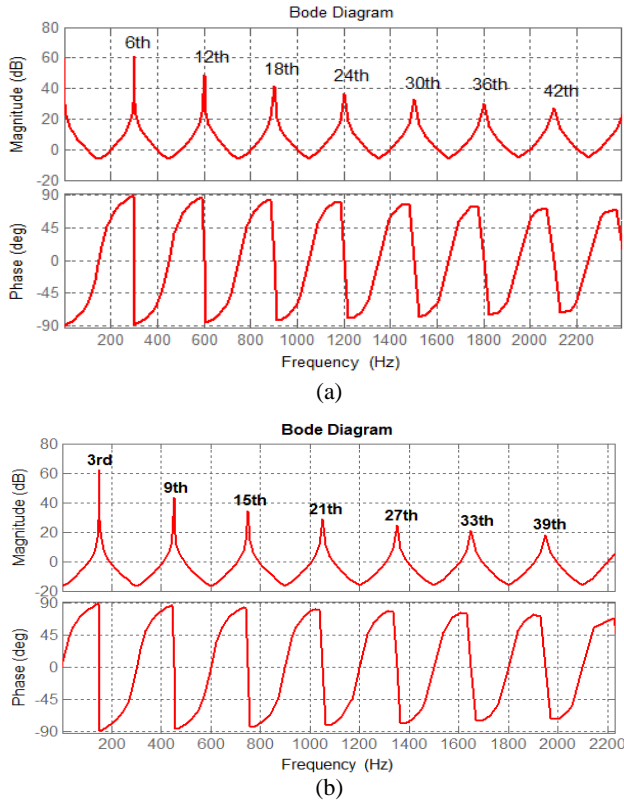
(a)

(b)

Fig. 5. Frequency response of (a) RC1 and (b) RC2.

conditions, an enhanced current controller with two RCs that have a delay time of $T_d = T_p/6$ is suggested. The block diagram of the proposed PI-2RC current controller is shown in Fig. 4, and the transfer functions of the two RCs, RC1 and RC2, are follows:

$$G_{RC1}(s) = \frac{K_r Q(s) e^{-sT_p/6}}{1 - Q(s) e^{-sT_p/6}}. \qquad (5)$$

$$G_{RC2}(s) = \frac{-K_r Q(s) e^{-sT_p/6}}{1 + Q(s) e^{-sT_p/6}}. \qquad (6)$$

Fig. 5 presents the frequency response in (5) and (6) with a fundamental frequency of 50 Hz. In Fig. 5(a), the RC1 designed in the d-q reference frame provides a high peak gain at the $6n$-th (n = 1, 2, 3…) harmonic orders, i.e., 300 Hz, 600 Hz, 900 Hz, and so on. Therefore, RC1 can effectively compensate $(6n \pm 1)$th (n = 1, 2, 3…) harmonics. Meanwhile, in Fig. 5(b), RC2 is designed to produce a high peak gain at the $(6n$-3)th (n = 1, 2, 3…) (triplen) harmonic orders, (i.e., 150 Hz, 450 Hz, 750 Hz, and so on). Therefore, it is able to compensate the $(6n$-3)th (n = 1, 2, 3…) harmonics. As a result, a combination of two RCs is sufficient to track all of the odd harmonics. Compared to the odd-harmonic RC developed in [21], the proposed RC provides a faster dynamic response due to the reduced time delay.
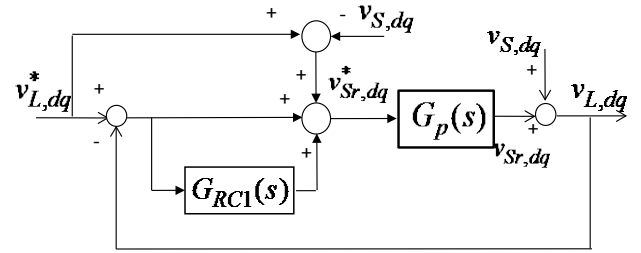
B. Voltage Controller for the Series APF

Fig. 6. Block diagram of the control scheme for the series APF.

Assume that the voltage available at the supply bus (v_S) is distorted and includes fundamental (v_{S1}) and harmonic components (v_{Sh}) as follows:

$$v_S = v_{S1} + v_{Sh} = V_{S1} \sin \omega t + \sum_{h \neq 1} V_{Sh} \sin(h\omega t - \theta_{sh}). \quad (7)$$

Similar to the control of the shunt APF, a simple approach is used to determine the reference voltage for the series APF so that the reference load voltage is directly generated in the d-q reference frame without a voltage sag detector or a harmonic detector as follows:

$$\begin{aligned} v_{Ld}^* &= V_{L1}^* \\ v_{Lq}^* &= 0 \end{aligned}, \qquad (8)$$

where $V_{L1}^* = \sqrt{2}.110\,\text{V}$ is the magnitude of the load voltage, which is a predetermined value. By generating the reference load voltage as in (8), the load voltage is always made to be sinusoidal with a predetermined constant magnitude of V_{L1}^*.

In order to properly control the load voltage to follow (8), the proposed voltage controller is designed in the d-q reference frame using a RC and a supply voltage feed-forward loop. In fact, the harmonic voltages in (7) in a three-phase system are mainly composed of the $(6n \pm 1)$th (n = 1, 2, 3...) harmonic orders. Hence, only these harmonics are considered and compensated in the voltage controller of the series APF. As a result, RC1, with the transfer function given in (5), is adopted for the voltage controller of the series APF. In addition, by adding a supply voltage feed-forward loop in the series APF control scheme in Fig. 6, the UPQC can effectively deal voltage sags without any additional voltage controllers.

III. FREQUENCY ADAPTIVE SCHEME FOR THE RC

For digital implementation, the transfer function of the PI controller and the RC in (3) and (5) are transformed into the discrete time domain by using the backward Euler discretization method as (9) and (10), respectively.

$$G_{PI}(z) = K_p + \frac{K_i T_s z}{z - 1}. \qquad (9)$$

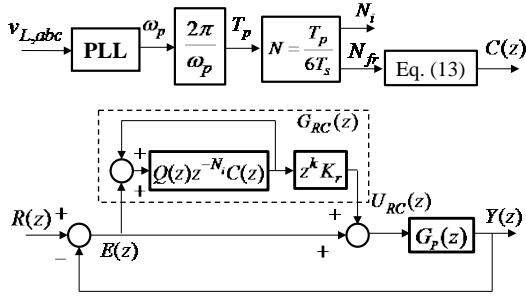$$G_{RC}(z) = \frac{K_r Q(z) z^{-N} z^k}{1 - Q(z) z^{-N}}. \qquad (10)$$

Fig. 7. Block diagram of the RC with frequency adaptive scheme.

Fig. 8. Frequency response of RC with different frequency adaptive techniques.

where $N = T_p / (6T_s)$ is the number of delay samples, which is an integer, T_s is the sampling period, and z^k is the phase lead term to compensate the phase lag caused by the plant $G_P(z)$.

As mentioned earlier, in practical systems, the grid frequency is not always constant, but may have small variations around its nominal value. For instance, with a nominal frequency of 50 Hz, power systems are regularly allowed to operate continuously with frequency deviations within the range from 49.5-50.5 Hz [36]. Then, if the grid frequency is different from the design frequency of the RC, the effectiveness of the RC is significantly diminished.

In order to maintain good performance of the RC despite frequency variations, a frequency-adaptive scheme is developed by using Padé's approximation, and it is applied to the RC as shown in Fig. 7. Compared to the previous frequency adaptive schemes such as the FIR filter [31], Linear or Lagrange interpolation [23]-[35], Padé's approximation is much simpler in structure, and it requires less computation. The other methods regularly need a high order function for an accurate approximation. However, a first or second order is sufficient with Padé's approximation [37].

To adapt to grid frequency variations, the proposed controller is composed of two parts: a phase-locked loop (PLL) and a fraction delay approximation algorithm. When the grid frequency changes, the grid frequency (ω_p) can be precisely detected through the PLL, whose algorithm is explained in [38]. Then, a fundamental period (T_p) is determined as $T_p = 2\pi / \omega_p$ and the number of delay samples, N, of the RC can be calculated as $N = T_p / (6T_s)$. Based on the number of delay samples N, the proposed RC can be implemented as (10). However, if N is a non-integer number due to grid frequency changes, the RC cannot be directly implemented in digital implementation. In order to solve this problem, the delay function $e^{-sT_p/6}$ in (5) and (6) is modified as:

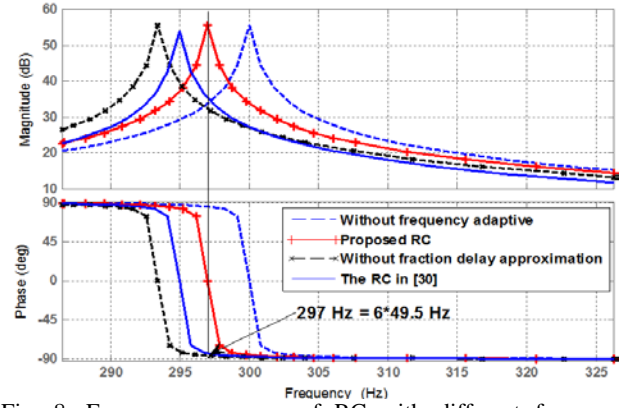$$e^{-sT_p/6} = e^{-NT_s s} = e^{-(N_i + N_{fr})T_s s} = e^{-N_i T_s s} e^{-N_{fr} T_s s} \quad ,(11)$$

where $N_i + N_{fr} = N$, with N_i and N_{fr} being the integer and fractional parts of N, respectively.

Since N_i is an integer, the term $e^{-N_i T_s s}$ can be easily implemented in the z-domain as z^{-N_i} . Meanwhile, since N_{fr} is a fractional number, $e^{-N_{fr}T_s s}$ cannot be directly implemented in the z-domain. Therefore, $e^{-N_{fr}T_s s}$ is approximated by using a first-order Padé's approximation [37]:

$$e^{-N_{fr}T_s s} \approx \frac{1 - \dfrac{N_{fr}T_s}{2}s}{1 + \dfrac{N_{fr}T_s}{2}s} = C(s) . \tag{12}$$

Transferring $C(s)$ into the z-domain by using backward Euler discretization, the delay function $C(z)$ is described as:

$$C(z) = \frac{(1 - N_{fr}) + (1 + N_{fr})z^{-1}}{(1 + N_{fr}) + (1 - N_{fr})z^{-1}} . \tag{13}$$

Finally, the transfer function of the proposed RC in the z-domain with the frequency-adaptive scheme is described as:

$$G_{RC}(z) = \frac{K_r Q(z)C(z)z^{-N_i}z^k}{1 - Q(z)C(z)z^{-N_i}} . \tag{14}$$

In order to investigate the effect of frequency variations on RCs, Fig. 8 shows the frequency responses nearby the 6th harmonics 300Hz at a nominal grid frequency of 50Hz for different kinds of RCs. These include the RC without a frequency adaptive scheme, the RC developed in [30], the RC without fraction delay approximation, and the proposed frequency RC. In this figure, it is assumed that the actual grid frequency is changed to 49.5 Hz from the nominal grid frequency, 50 Hz, and the 6th harmonic frequency is changed from 300 Hz (sixth of 50Hz) to 297 Hz (sixth of 49.5Hz). From Fig. 8, for the RC without a frequency adaptive scheme, the peak gain at 297 Hz is significantly reduced to 30 dB compared to the original peak gain (55 dB) because the peak gain remains at 300 Hz without compensation. Similarly, the peak gains of the other methods, except the proposed RC,
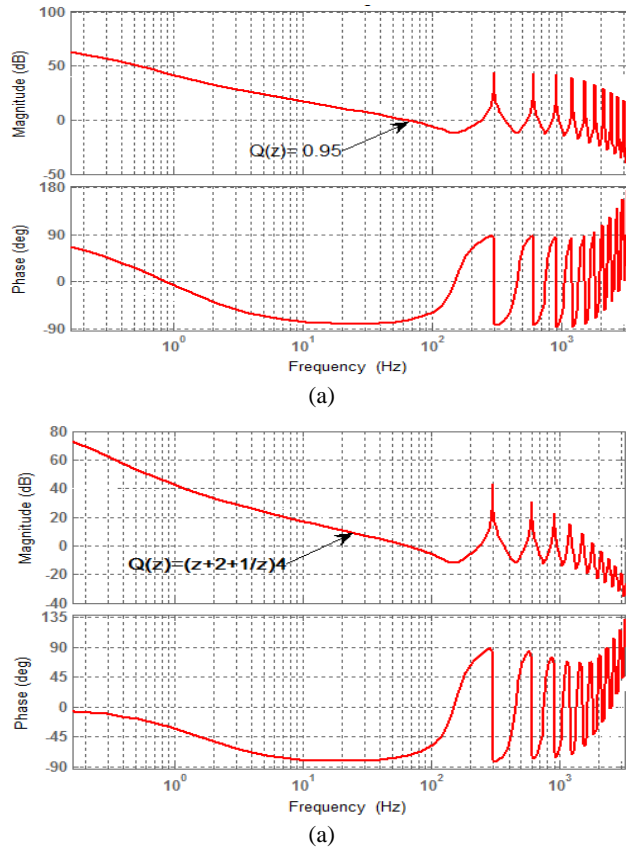
(a)

(a)

Fig. 9. Frequency response of the open-loop transfer function of the PI-RC controller with (a) $Q(z) = 0.95$ and (b) $Q(z) = (z + 2 + z^{-1})/4$.

also are not located at the changed frequency, 297 Hz. Therefore, the effectiveness of the RCs is dramatically degraded when the grid deviates from its nominal value (50 Hz). In contrast, the proposed RC with the frequency adaptive scheme has exactly the peak gain at the sixth of 49.5 Hz, so that the proposed control scheme can maintain a good performance regardless of grid frequency deviations.

IV. DESIGN OF REPETITIVE CONTROLLERS

A. Design of the RC for the Series APF

In order to design the RC in (14), three components are considered: the filter $Q(z)$, the phase lead term z^k, and the RC controller gain K_r. Among these three components, the filter $Q(z)$, that is used to improve the system stability by reducing the peak gain of the RC at a high frequency range, has to be determined first. Afterward, the phase lead term z^k is designed to compensate the phase lag caused by the control plant to achieve better harmonic compensation performance of the RC. Finally, the controller gain of the RC, K_r is chosen based on the system stability condition in (17).

1) Selection of the filter $Q(z)$: $Q(z)$ is used to improve system stability by reducing the peak gain of the RC at the high

frequency range. There are two popular methods that have been used in previous studies to employ $Q(z)$: a closed unity gain $Q(z) = 0.95$, and a zero-phase LPF $Q(z) = (z + 2 + z^{-1})/4$ [20], [21]. In this study, these two types of $Q(z)$ are adopted, and the frequency responses of the RC for both types of $Q(z)$ are plotted in Fig. 9 in order to determine a suitable $Q(z)$ for the RC. In Fig. 9(a), when $Q(z)=0.95$, the RC provides a high gain over the entire frequency range. As a result, the system becomes unstable due to the high gain at the high frequency region. In contrast, in Fig. 9(b), with $Q(z) = (z + 2 + z^{-1})/4$, the gain of the RC is high at the low order harmonics. However, it reduces to significantly less than 0 dB at the high frequency range (higher than 2 kHz). It is well-known that a low peak gain at the high frequency range can ensure a robust system. Furthermore, in contrast to the typical first order LPF, the zero-phase LPF does not shift to the original position of the RC peak gain. Therefore, the use of this zero-phase LPF does not affect the RC accuracy. Thus, $Q(z) = (z + 2 + z^{-1})/4$ was chosen for this study.

2) Determination of the Phase Lead Term z^k : Because the control plant $G_p(z)$ commonly acts a low-pass filter, which introduces some phase lag, a phase lead term z^k is needed to compensate the phase lag of $G_p(z)$, and k is selected to minimize the phase displacement of $G_p(z)z^k$, where the transfer function of inductor L_{sh} in the continuous and discrete time domains are given as:

$$G_p(s) = \frac{1}{L_{sh}s + R_{sh}}$$

$$G_p(z) = \frac{T_s}{(L_{sh} + R_{sh}T_s) - L_{sh}z^{-1}}. \tag{15}$$

Fig. 10 shows the frequency response of $G_p(z)z^k$ with different values of k. From Fig. 10, $k=5$ is selected because it provides a minimum phase displacement near the dominant harmonics, such as the 5th, 7th, 11th and 13th, and the system stability is guaranteed up to the 37th harmonic component at a frequency of 1.85 kHz. According to [20], the phase displacement of $G_p(z)z^k$ should not exceed the limitation $[-90°; 90°]$ in order to ensure that the system is stable. Furthermore, to remove the effect of the delay time due to the digital control in the experimental implementation, $k=6$ is used.

3) Determination of the Controller Gain K_r: In order to investigate the stability condition of the RC and to determine the controller gain K_r, the tracking error of the RC with respect to the reference value is derived from Fig. 3 as:
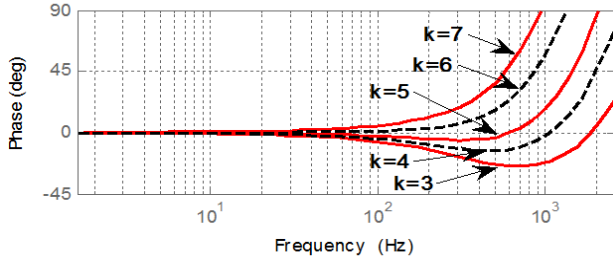
Fig. 10. Phase lag compensation with different values of *k*.
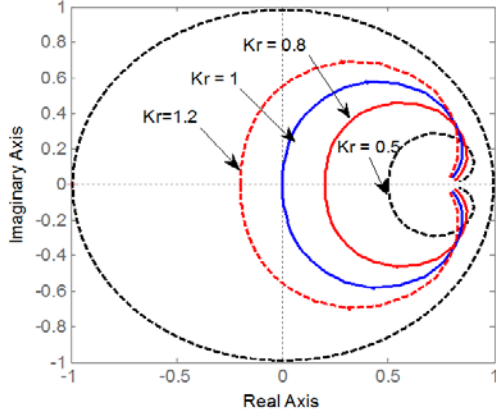
Fig. 11. Loci of the vector $H(e^{j\omega T_s})$.

$$E(z) = \frac{[1 - Q(z)z^{-N}][1 - G_p(z)]}{1 - z^{-N}[Q(z) - K_r z^k G_p(z)]} R(z) . \qquad (16)$$

Let $H(z) = Q(z) - K_r z^k G_p(z)$. Based on the small gain theorem [19], the repetitive control system is sufficiently stable if the vector $H(e^{j\omega T_s})$ is located within the unity circle. Consequently, the stability condition of the repetitive control system is given as:

$$\left| H(e^{j\omega T_s}) \right| < 1 , \qquad (17)$$

$\omega \in [0, \pi / T_s]$; where π / T_s is the Nyquist frequency.

The loci of the vector $H(e^{j\omega T_s})$ are plotted in Fig. 11 with respect to different values of K_r and the controller gain K_r is selected based on the stability condition given in (17). It can be observed that the vector $H(e^{j\omega T_s})$ is located inside the unity circle, i.e., the system is stable if K_r is less than 1.2. In fact, a large K_r offers a better steady-state performance as well as a faster response. However, it also limits the stability margin of the system. Therefore, in order to guarantee a sufficient stability margin, K_r=0.8 is selected.

B. Design of the RC for the Series APF

The design of the RC for the series APF is similar to that of the shunt APF. In terms of the filter $Q(z)$, the zero phase-shift LPF $Q(z) = (z + 2 + z^{-1})/4$ is also selected.

The next step is to determine the phase lead term z^k to
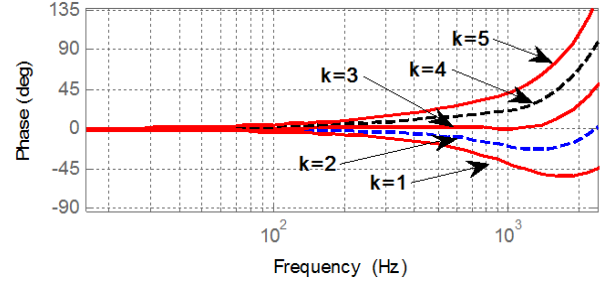
Fig. 12. Phase lag compensation with different values of *k*.
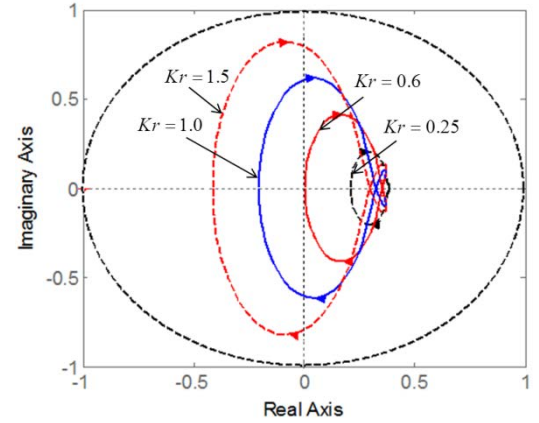
Fig. 13. Loci of the vector $H(e^{j\omega T_s})$.

compensate the phase lag caused by $G_p(z)$. The plant of the series APF is the *LC* filter with the transfer functions in continuous and discrete time domains defined as;

$$G_p(s) = \frac{1}{L_f C_f s^2 + R_f C_f s + 1}$$

$$G_p(z) = \frac{1}{L_f C_f (\frac{1 - z^{-1}}{T_s})^2 + R_f C_f (\frac{1 - z^{-1}}{T_s}) + 1} . \qquad (18)$$

The frequency response of $G_p(z) z^k$ is illustrated in Fig. 12 with different values of *k*. From Fig. 12, *k*=3 is chosen. This can minimize the phase displacement of $G_p(z) z^k$. Moreover, to remove the impact of the delay time due to the digital control, *k*=4 is selected in practice implementation.

Similar to Fig. 11, the controller gain K_r for the RC in the series APF is also determined based on the loci of the vector $H(e^{j\omega T_s})$ as shown in Fig. 13. From Fig. 13, K_r=1 is selected.

V. EXPERIMENTAL RESULTS

In order to validate the effectiveness of the proposed control strategy, an experimental system was built in the laboratory as shown in Fig. 14. The system parameters for the whole system are given in the Appendix. The control strategy
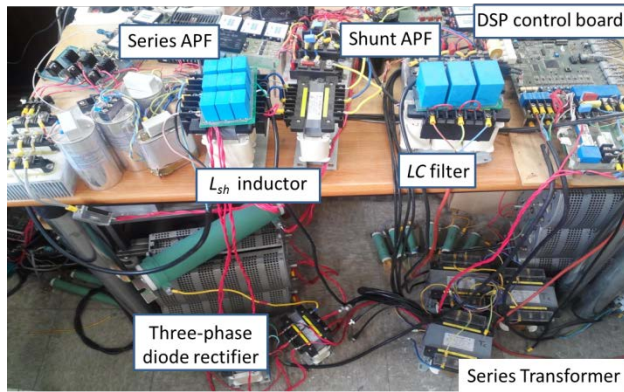
Fig. 14. Experimental platform of three-phase UPQC.

is implemented using a 32-bit fixed-point DSP (TMS320F2812 of Texas Instruments). The sampling and switching frequencies are set to 9 kHz so that $N = 30$ at a nominal grid frequency of 50 Hz. The supply voltage is generated by a Programmable AC Power Source (Chroma 61704), and a three-phase diode rectifier is used as the nonlinear load. The total harmonic distortion (THD) values of the load voltage and the supply current are measured by a power analyzer (HIOKI 3193). The supply voltage v_{Sa} is programmed to have a total harmonic distortion (THD) of 8.61%, and the load current i_{La} is distorted due to a nonlinear load with a high THD of 25.2% that is caused by the three-phase diode rectifier.

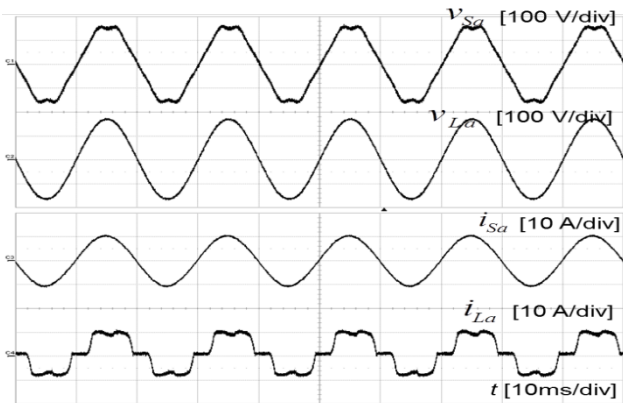### A. Steady-State Performance of the Voltage and Current Harmonic Compensation

Fig. 15 shows the harmonic compensation performance of the UPQC by using the traditional PI controller in Fig. 15(a), which is one of the traditional controllers; the PI controller plus multiple resonant controllers in Fig. 15(b), which is one of the advanced controllers; and the proposed control strategy in Fig. 15(c). As shown in Fig. 15(a), by using only the PI controller, harmonic compensation cannot be achieved. The load voltage and the supply current are far from sinusoidal waveforms. On the other hand, even though the load voltage and the supply current are effectively compensated through the PI controller plus multiple resonant controllers and the proposed control methods in Fig. 15(b) and 15(c), respectively, they have a small difference in their performance. As investigated in the RC characteristic, one single RC can simultaneously compensate a large number of harmonic components. Meanwhile, due to the long computation time of the resonant controller, the control method in [17] can add three resonant controllers with the maximum harmonic order up to the 19th order. For this reason, the proposed control algorithm provides a better control performance compared to the PI controller plus multiple resonant controllers with lower values for the THD of the load voltage and supply current as shown in Table I. In addition, from Table I, the proposed
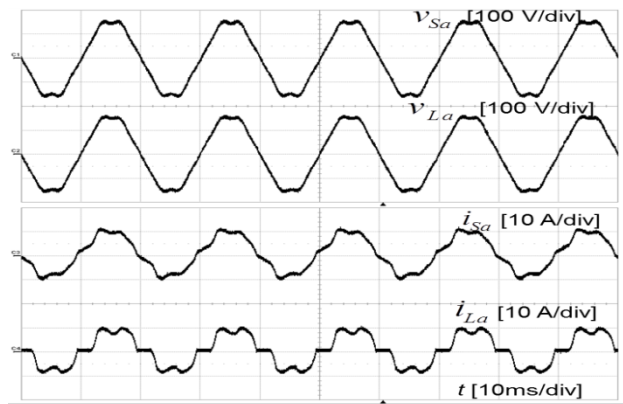

(a)
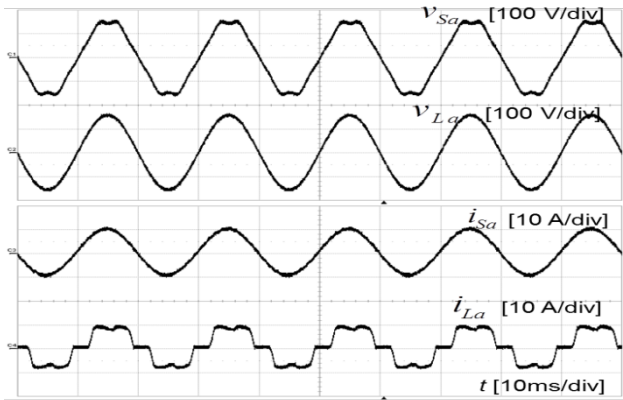
(b)

(c)

Fig. 15. Steady-state performance of the UPQC by using (a) PI controller, (b) PI-3R controller, and (c) Proposed controller.

TABLE I
COMPARISON OF THE HARMONIC COMPENSATION PERFORMANCE AND CALCULATION TIME OF THE DIFFERENT CONTROL STRATEGIES

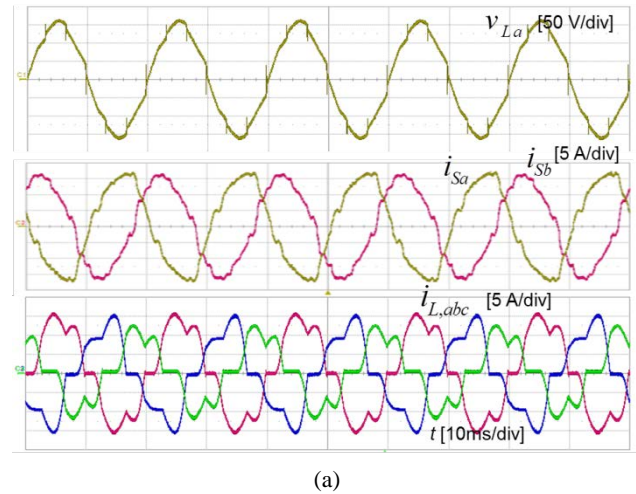|	PI controller	PI-3R controller [17]	Proposed controller
THD of v_{La}	6.37 %	1.27 %	0.64 %
THD of i_{Sa}	12.7 %	3.65 %	1.57 %
Calculation time	41 µs	95 µs	51 µs
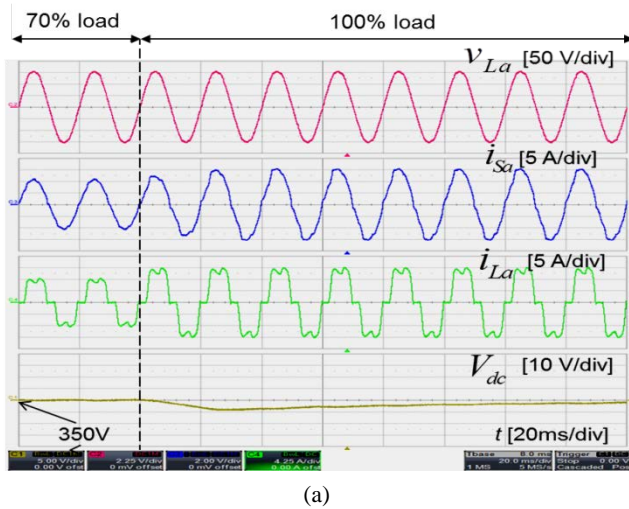
(a)
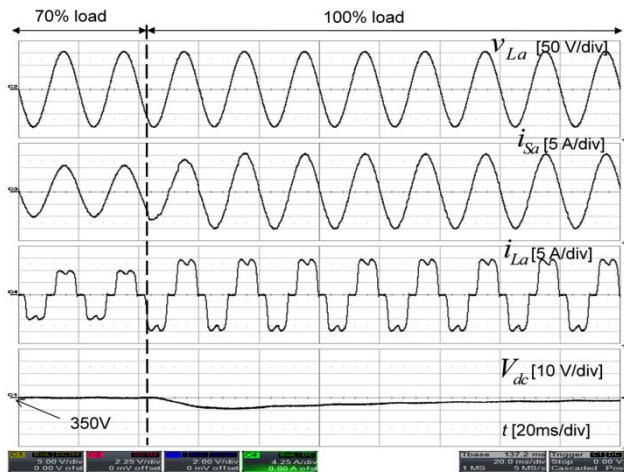
(b)

Fig. 16. Dynamic response of the UPQC under load current change with (a) the traditional RC and (b) the proposed RC.

(a)

(b)

Fig. 17. Experimental results of the UPQC under nonlinear and unbalanced load conditions using (a) the RC deveoped in [24] and (b) the proposed RC.
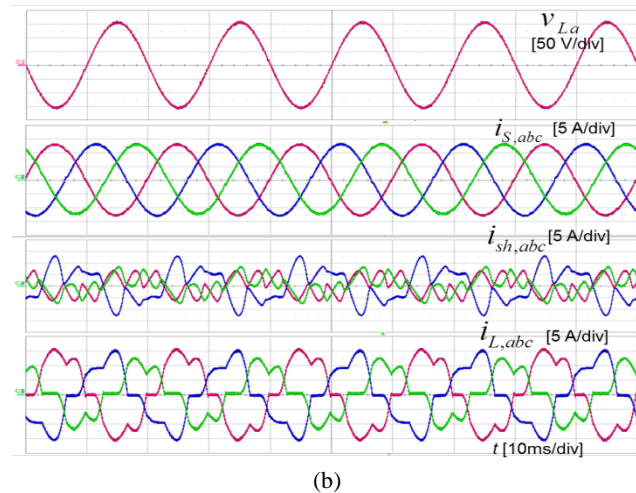
control method needs a much shorter computation time compared to the multiple resonant controller solution. Therefore, the proposed control algorithm is simpler and more effective compared to the other control methods. These results verify the effectiveness of the proposed control strategy for voltage and current harmonics compensation.

B. Dynamic Response of the Current Harmonics Compensation under Load Changes

To demonstrate the fast dynamic response of the proposed control method for the UPQC under load variations, an experimental test on the UPQC with a load change is carried out. In this test, the supply voltage is the same as that in the steady state test, while the nonlinear load current has a step change from 70% load to the full load condition. The experimental results are shown in Fig. 16, where the load voltage, supply current, load current, and DC-link voltage are plotted. From Fig. 16(a), it can be observed that the dynamic response of the traditional RC is very poor when the load changes. Even after a long period of time, about 160ms, the

supply current has not settled down into the new steady-state condition (sinusoidal waveform). In contrast, by using the proposed RC, the supply current reaches the new steady-state condition in a short time, about 20ms. These results clearly verify the fast transient characteristic of the proposed RC. In Fig. 16, even though the DC-link voltage does not recover quickly, the voltage reduction is very small (only 10 V), and it has no effect on the operation of the UPQC.

C. Performance of the Proposed Control Strategy under Unbalanced and Nonlinear Loads

Fig. 17(a) shows experimental result of the UPQC by using the RC introduced in [24] under nonlinear and unbalanced load condition, where a single-phase diode rectifier is connected between phases "a" and "b" to create an unbalanced load condition. In Fig. 17(a), it can be observed that both the load voltage and the supply currents cannot be compensated to be sinusoidal because the RC developed in [24] only tracks the $(6n \pm 1)$th ($n = 1, 2, 3…$) harmonics. As a result, the RC cannot deal with the triplen harmonics
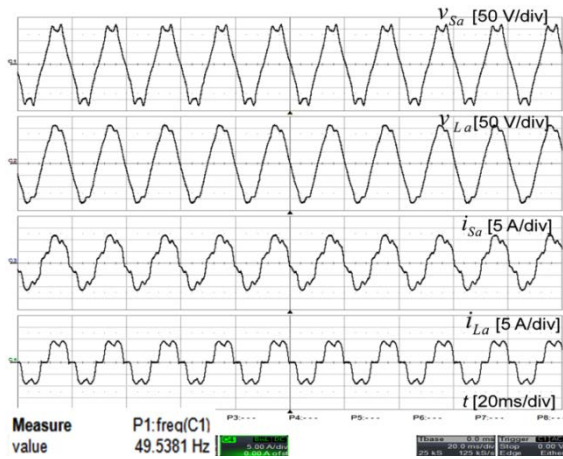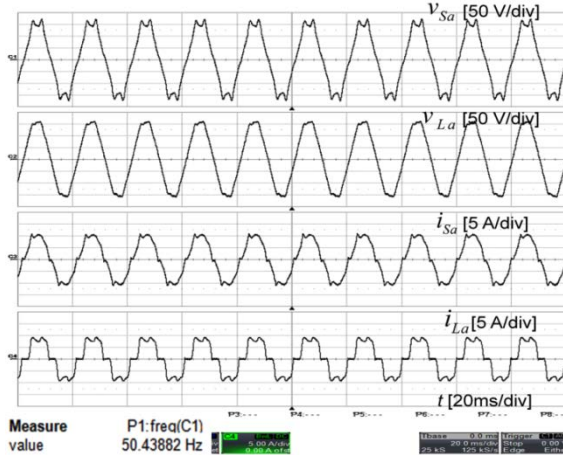
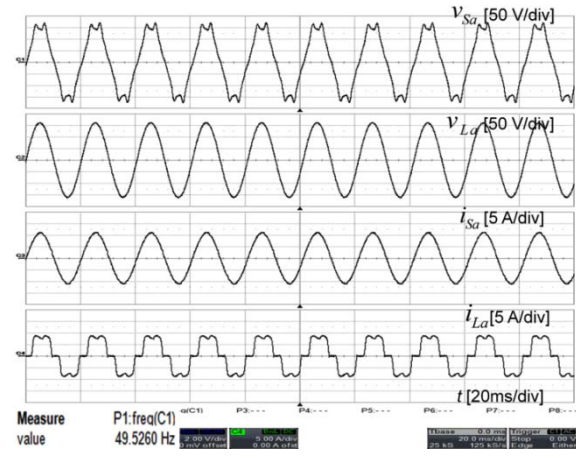Fig. 18. Experimental results of UPQC without adaptive-frequency scheme at (a) 49.5 Hz, (b) 50.5 Hz.

Fig. 19. Experimental results of UPQC with adaptive-frequency scheme at (a) 49.5 Hz, (b) 50.5 Hz.
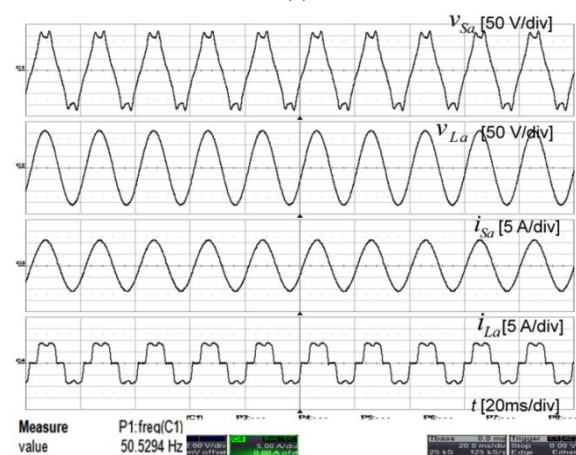
generated by the unbalanced load. Therefore, the RC in [24] cannot provide good harmonic compensation performance under unbalanced and nonlinear loads. In contrast, as presented in Fig. 17(b), by using the proposed control algorithm, the load voltage and the supply currents are effectively compensated to be sinusoidal and balanced even though the load currents are distorted and unbalanced. This is because the proposed current controller is developed to track the ($6n$-3)th ($n = 1, 2, 3…$) (triplen) along with the ($6n \pm 1$)th ($n = 1, 2, 3…$) harmonics with two RCs. As a result, it can effectively compensate all odd harmonic currents generated by loads. These results verify the feasibility of the proposed control strategy. It can effectively compensate harmonic currents generated from unbalanced load and nonlinear loads.

D. Performance of the Voltage and Current Harmonic Compensation under Grid Frequency Deviations

In Figs. 15-17, the UPQC with the proposed control strategy was shown to provide good compensation performance at a nominal grid frequency of 50 Hz. However, in practice, the grid frequency is not always constant, but may have small variations around the nominal value. Fig. 18

shows the effects of grid frequency deviations without the frequency-adaptive scheme. The performance of the UPQC at a grid frequencies of 49.5 Hz and 50.5 Hz are shown in Figs. 18(a) and 18(b), respectively. As can be seen, under the condition where the frequency-adaptive scheme is not adopted, the performance of the UPQC significantly deteriorates when the grid frequency deviates from the nominal frequency of 50Hz. In contrast, as shown in Fig. 19, thanks to the effectiveness of the frequency-adaptive scheme, the compensating performance of the UPQC does not deteriorate despite the grid frequency deviations. The load voltage and the supply current are still compensated to be sinusoidal with very low THD values.

Table II shows a summary of the THD values for the load voltage and the supply current both with and without the frequency-adaptive scheme. As indicated in Table II, under grid frequency changes, the good performance of the UPQC is difficult to maintain without the frequency-adaptive scheme. In contrast, under the proposed frequency-adaptive scheme, the THD values of the load voltage and the supply current are kept extremely low. They are less than 1% and

TABLE II
PERFORMANCE OF THE UPQC WITH AND WITHOUT THE
FREQUENCY-ADAPTIVE SCHEME

	Without frequency-adaptive scheme			With frequency-adaptive scheme		
Frequency (Hz)	49.5	50	50.5	49.5	50	50.5
THD of v_{La} (%)	5.49	0.64	4.35	0.88	0.64	0.77
THD of i_{Sa} (%)	16.65	1.57	12.45	1.75	1.57	1.63

2%, respectively, and are completely compliant with the IEEE 519-1992 standards [39].

VI. CONCLUSION

In this paper, a simplified UPQC control system was proposed by using a modified RC which has a fast transient response and grid frequency adaptive capability along with excellent steady-state performance. The UPQC with the proposed control approach is able to effectively compensate both the load voltage and the supply current to be sinusoidal regardless of voltage distortions in the supply side and nonlinear/unbalanced loads. In addition, owing to the frequency-adaptive scheme in the RC, an excellent compensation performance of the UPQC is maintained in spite of grid frequency deviations. The whole control strategy was implemented using a TMS320F2812 DSP and the effectiveness of the proposed control method was verified through experimental results. They show that he load voltage and the supply current are compensated to be sinusoidal, with THD values of less than 1% and 2%, respectively, in all test cases. Despite its simplified controller configuration, the proposed control method provides a better control performance compared to other control strategies.

APPENDIX

SYSTEM PARAMETERS

	Parameters		Value
Supply	Fundamental voltage	V_{l-l}	190 V (l-l RMS)
	Nominal grid frequency	f_s	50 Hz
	5th harmonic voltage		7%
	7th harmonic voltage		5%
Loads	Diode rectifier load	R_{dc}	20 Ω
	Three-phase linear load	R_L	50 Ω
DC-link	Reference voltage	V_{dc}^*	350 V
	Capacitance	C_{dc}	2.5 mF
Shunt APF	Filter inductance	L_{sh}	2 mH
	Filter resistance	R_{sh}	0.1Ω
Series APF	LC filter inductance	L_f	0.5 mH
	LC filter capacitance	C_f	12 μF
	Damping resistance	R_f	0.5Ω
	Sampling/switching frequency	f_{sw}	9 kHz

REFERENCES

[1] Q. Liu, L. Peng, Y. Kang, S. Tang, D. Wu, and Y. Qi, "A novel design and optimization method of an LCL filter for a shunt active power filter, "*IEEE Trans. Ind. Electron.*, Vol. 61, No. 8, pp. 4000-4010, Aug. 2014.

[2] Q. Trinh and H. Lee, "An advanced current control strategy for three phase shunt active power filters," *IEEE Trans. Ind. Electron.*, Vol. 60, No. 12, pp. 5400-5410, Dec. 2013.

[3] S. Rahmani, A. Hamadi, K. Al-Haddad, and L. A. Dessaint, "A combination of shunt hybrid power filter and Thyristor-controlled reactor for power quality," *IEEE Trans. Ind. Electron.*, Vol. 61, No. 5, pp. 2152-2164, May 2014.

[4] H. Awad, H. Nelsen, F. Blaabjerg, and M. John Newman, "Operation of static series compensator under distorted utility conditions," *IEEE Trans. Power Syst.*, Vol. 20, No. 1, pp. 448-457, Feb. 2005.

[5] Y. W. Li, F. Blaabjerg, D. M. Vilathgamuwa, and P. C. Loh, "Design and comparison of high performance stationary-frame controllers for DVR implementation," *IEEE Trans. Power. Electron.*, Vol. 22, No. 2, pp. 602-612, Mar. 2007.

[6] H. Fujita and H. Akagi, "The unified power quality conditioner: The integration of series and shunt active filters," *IEEE Trans. Power Electron.*, Vol. 13, No. 2, pp. 315-322, Mar. 1998.

[7] H. Akagi, E. H. Watanabe, and M. Aredes, *Instantaneous Power Theory and Applications to Power Conditioning. Hoboken*, NJ: Wiley-IEEE Press, Apr. 2007.

[8] V. Khadkikar, "Enhancing electric power quality using UPQC: A comprehensive overview," *IEEE Trans. Power Electron.,* Vol. 27, No. 5, pp. 2284-2297, May 2012.

[9] K. H. Kwan, Y. C. Chu, and P. L. So, "Model-based H∞ control of a unified power quality conditioner," *IEEE Trans. Ind. Electron.*, Vol. 56, No. 7, pp. 2493-2504, Jul. 2009.

[10] K. H. Kwan, P. L. So, and Y.-C. Chu, "An output regulation-based unified power quality conditioner with Kalman filters," *IEEE Trans. Ind. Electron.*, Vol. 59, No. 11, pp. 4248-4262, Nov. 2012.

[11] M. Kesler and E. Ozdemir, "Synchronous reference frame based control method for UPQC under unbalanced and distorted load conditions," *IEEE Trans. Ind. Electron.*, Vol. 58, No. 9, pp. 3967-3975 , Sep. 2011.

[12] V. Khadkikar, A. Chandra, A. O. Barry, and T. D. Nguyen, "Power quality enhancement utilizing single phase unified power quality conditioner: Digital signal processor-based experimental validation," *IET Power Electronics*, Vol. 4, No. 3, pp. 323-331, Mar. 2011.

[13] M. Basu, S. P. Das, and G. K. Dubey, "Investigation on the performance of UPQC-Q for voltage sag mitigation and power quality improvement at a critical load point," *IET Generation, Transmission & Distribution*, Vol. 2, No. 3, pp.414-423, Jul. 2008.

[14] I. Axente, M. Basu, M. F. Conlon, and K. Gaughan, "A 12-kVA DSP-controlled laboratory prototype UPQC capable of mitigating unbalance in source voltage and load current," *IEEE Trans. Power Electron.*, Vol. 25, No. 6, pp.

1302-1309, Jun. 2010.

[15] V. G. Kinhal, P. Agarwal, and H. O. Gupta, "Performance investigation of neural-network-based unified power-quality conditioner," *IEEE Trans. Power Del.*, Vol. 26, No. 1, pp. 431-437, Jan. 2011.

[16] S. B. Karanki, M. K. Mishra, and B. K. Kumar, "Particle swarm optimization-based feedback controller for unified power-quality conditioner," *IEEE Trans. Power Del.*, Vol. 25, No. 4, pp. 2814-2824, Oct. 2010.

[17] Q.-N. Trinh and H.-H. Lee, "Novel control strategy for a UPQC under distorted source and nonlinear load conditions," *Journal of Power Electronics*, Vol. 13, No. 1, pp. 161-169, Jan. 2013.

[18] A. G. Yepes, F. D. Freijedo, O. Lopez, J. Malvar, and J.Doval-Gandoy, "High-performance digital resonant controllers implemented with two integrators," *IEEE Trans. Power Electron.*, Vol. 26, No. 2, pp. 1692-1712, Feb. 2011.

[19] K. Zhang, Y. Kang, J. Xiong, and J. Chen, "Direct repetitive control of SPWM inverters for UPS purpose," *IEEE Trans. Power Electron.*, Vol. 18, No. 3, pp. 784-792, May 2003.

[20] B. Zhang, D. Wang, K. Zhou, and Y. Wang, "Linear phase lead compensation repetitive control of a CVCF PWM inverter," *IEEE Trans. Ind. Electron.*, Vol. 55, No. 4, pp. 1595-1602, Apr. 2008.

[21] K. Zhou, K.-S. Low, Y. Wang, F.-L. Luo, B. Zhang, and Y. Wang, "Zero-phase odd-harmonic repetitive controller for a single-phase PWM inverter," *IEEE Trans. Power Electron.*, Vol. 21, No. 1, pp. 193-201, Jan. 2006.

[22] Y. Cho and J.-S. Lai, "Digital plug-in repetitive controller for single-phase bridgeless PFC converters," *IEEE Trans. Power Electron.*, Vol. 28, No. 1, pp. 165-175, Jan. 2013.

[23] Z. Zou, Z. Wang, and M. Cheng, "Modeling, analysis, and design of multifunction grid-interfaced inverters with output LCL filter," *IEEE Trans. Power Electron.*, Vol. 29, No. 7, pp. 3830-3839, Jul. 2014.

[24] Q. N. Trinh and H. H. Lee, "An advanced repetitive controller to improve the voltage characteristics of distributed generation with nonlinear loads," *Journal of Power Electronics,* Vol. 13, No. 3, pp. 409-418, May 2013.

[25] D. Chen, J. Zhang, and Z. Qian, "Research on fast transient and 6n ± 1 harmonics suppressing repetitive control scheme for three-phase grid-connected inverters," *IET Power Electronics*, Vol. 6, No. 3, pp. 601-610, Mar. 2013.

[26] Z. Zeng, J.-Q. Yang, S.-L. Chen, and J. Huang, "Fast-transient repetitive control strategy for a three-phase LCL filter-based shunt active power filter," *Journal of Power Electronics*, Vol. 14, No. 2, pp. 392-401, Mar. 2014.

[27] M. A. Herran, J. R. Fischer, S. A. Gonzalez, M. G. Judewicz, I. Carugati, and D. O. Carrica, D.O., "Repetitive control with adaptive sampling frequency for wind power generation systems," *IEEE Journal of Emerging and Selected Topics in Power Electronics*, Vol. 2, No. 1, pp. 58-69, Mar. 2014.

[28] J. Olm, G. Ramos, and R. Costa-Castello, "Stability analysis of digital repetitive control systems under time-varying sampling period," *IET Control Theory & Applications*, Vol. 5, No. 1, pp. 29-37, Jun. 2011.

[29] T. Hornik and Q.-C. Zhong, "H$^\infty$ repetitive voltage control of grid connected inverters with a frequency adaptive mechanism," *IET Power Electronics*, Vol. 3, No. 6, pp. 925-935, Nov. 2010.

[30] D. Chen, J. Zhang, and Z. Qian, "An improved repetitive control scheme for grid-connected inverter with frequency-adaptive capability," *IEEE Trans. Ind. Electron.*, Vol. 60, No. 2, pp. 814-823, Feb. 2013.

[31] M. Rashed, C. Klumpner, and G. Asher, "Repetitive and resonant control for a single-phase grid-connected hybrid cascaded multilevel converter," *IEEE Trans. Power Electron.,* Vol. 28, No. 5, pp. 2224-2234, May 2013.

[32] Z. Zou, K. Zhou, Z. Wang, and M. Cheng, "Fractional-order repetitive control of programmable AC power sources," *IET Power Electronics*, Vol. 7, No. 2, pp. 431-438, Feb. 2014.

[33] G. Escobar, M. Hernandez-Gomez, A. A. Valdez-Fernandez, M. Lopez-Sanchez, and G. A. Catzin-Contreras, "Implementation of a 6n±1 repetitive controller subject to fractional delays," *IEEE Trans. Ind. Electron.*, to be published.

[34] Y. Wang; D. Wang, B. Zhang, and K. Zhou, "Fractional delay based repetitive control with application to PWM DC/AC converters," *Control Applications, 2007. CCA 2007. IEEE International Conference on*, pp. 928-933, 2007.

[35] M. H. J. Bollen, *Understanding Power Quality Problems: Voltage Sags and Interruptions*, New York: IEEE Press, 1999.

[36] G. J. Silva, A. Datta, S. P. Bhattacharyya, *PID Controllers for Time delay Systems*, Birkhäuser, 2004.

[37] F. D. Freijedo, J. Doval-Gandoy, O. Lopez, and E. Acha, "Tuning of phase locked loops for power converters under distorted utility conditions," *IEEE Trans. Ind. Appl.*, Vol. 45, No. 6, pp. 2039-2047, Nov./Dec. 2009.

[38] IEEE Recommended Practices and Requirements for Harmonic Control in Electrical Power Systems, IEEE Std. 519-1992, 1992.

Quoc-Nam Trinh was born in Vietnam, in 1985. He received his B.S. degree in Power Engineering from the Ho Chi Minh City University of Technology, Ho Chi Minh City, Vietnam, in 2008, and his Ph.D. degree in Electrical Engineering from the University of Ulsan, Ulsan, Korea, in 2014. Since August 2014, he has been with the Energy Research Institute @ NTU, Nanyang Technological University, Singapore, as a Postdoctoral Research Fellow. His current research interests include active power filters, harmonic compensation, distributed generation, and grid-connected inverters.

Hong-Hee Lee received his B.S., M.S., and Ph.D. degrees in Electrical Engineering from Seoul National University, Seoul, Korea, in 1980, 1982, and 1990, respectively. From 1994 to 1995, he was a Visiting Professor at Texas A&M University, College Station, TX, USA. He has been a Professor in the School of Electrical Engineering, Department of Electrical Engineering, University of Ulsan, Ulsan, Korea, since 1985. He is also the Director of the Network-based Automation Research Center (NARC), University of Ulsan, which is sponsored by the Ministry of Trade, Industry and Energy, Korea. His current research interests include power electronics, network-based motor control, and renewable energy. Dr. Lee is a member of the Institute of Electrical and Electronics Engineers (IEEE), the Korean Institute of Power Electronics (KIPE), the Korean Institute of Electrical Engineers (KIEE), and the Institute of Control, Robotics and Systems (ICROS).